RSC Advances

Kinetic exploration appended by Spectroscopic and Molecular Docking analysis in search of an optimal condition for effective degradation of Malachite Green

Journal:	*RSC Advances*
Manuscript ID:	RA-ART-03-2015-004724.R1
Article Type:	Paper
Date Submitted by the Author:	04-Apr-2015

Complete List of Authors:	Dasmandal, Somnath; Jadavpur University, Chemistry Mandal, Harasit; Jadavpur University, Chemistry Rudra, Suprna; Jadavpur University, Chemistry Kundu, Arjama; Jadavpur University, Chemistry Majumdar, Tapas; University of Kalyani, Chemistry Mahapatra, Prof. Ambikesh; Jadavpur University, Dept. of Chemistry

Kinetic exploration appended by Spectroscopic and Molecular Docking analysis in search of an optimal condition for effective degradation of Malachite Green

Somnath Dasmandal[a], Harasit Kumar Mandal[a], Suparna Rudra[a], Arjama Kundu[a], Tapas Majumdar[b] and Ambikesh Mahapatra[a,*]

[a]*Department of Chemistry, Jadavpur University, Kolkata 700 032, India*

[b]*Department of Chemistry, University of Kalyani, Kalyani 741 235, India*

*Corresponding author. Tel.: +9133 2457 2770 (office), +9133 2432 4586 (residence); fax: +9133 2414 6223.

E-mail addresses amahapatra@chemistry.jdvu.ac.in, ambikeshju@gmail.com

Abstract

The degradation of malachite green (MG) by alkaline hydrolytic process has been explored spectrophotometrically. The kinetics of the reaction have been meticulously studied under the influence of cationic alkyltrimethylammonium bromide (DTAB, TTAB and CTAB) surfactants; α-, β- and γ-cyclodextrins (CDs) and surfactant–β-CD mixed systems applying pseudo-first order condition at 298 K. The surfactants and cyclodextrins individually catalyze the hydrolytic rate, whereas surfactant–β-CD mixed systems exhibit both inhibiting and catalytic influence depending on the surfactant concentrations. The kinetic results have been explained precisely based on pseudo-phase ion exchange (PIE) model of micelles and CD-catalyzed model of CD systems. The surfactants exhibit micellar surface catalysis, while CDs accelerate the rate by forming MG–CD inclusion complexes, thereby facilitating the nucleophilic attack of its ionized secondary hydroxyl group to carbocation center of MG. The encapsulation of MG within the supramolecular host cavity of the CDs has been investigated diligently using steady-state absorption spectroscopic technique. The result shows 1:1 host–guest complexation with different relative orientations of the guest (MG) inside the hosts. The studies employing density functional theory (DFT) as well as molecular docking analysis provide valuable insights on the insertion mechanism. The results reveal that quantitative analysis can be utilized to predict an optimum condition for the fastest degradation of MG in ambient environments.

Keywords: kinetics, micellar catalysis, host-guest complexation, DFT, molecular docking.

1. Introduction

The chemistry of dyes and their applications in various scientific fields gets immense attention in the modern times. Malachite green (MG) is an important dye of commercial and analytical importance [1]. However, the high solubility of the dye in water makes them potential water pollutants. The contamination of the dye to water-systems puts forward a severe risk to the aquatic living organisms through bioaccumulation and thus entering into the food chain. Thus the removal of the dye from industrial effluents in an economic fashion is the leading challenge. A number of methods have recently been used for dealing with the treatment of wastewater discharged from textile industries *viz*., physico-chemical treatment by biological oxidation, adsorption and advanced oxidation processes (AOPs), e.g., ozonation, photolysis, electrochemical, sonolysis etc [2,3]. Usually, these processes have been found to release of more toxic products than the parent compound that prove fatal for the living creatures [4]. Hydrolysis is one of the prime detoxification mechanisms of organic compounds as the hydrolysis by-products are normally less toxic to the environment than the parent compound [5]. Thus in our present study we have extensively studied the kinetics of alkaline hydrolysis of malachite green in different microheterogeneous environments made up of surfactants, cyclodextrins and their mixed systems.

The microenvironments consists of surfactants are capable of both catalyzing and inhibiting the hydrolysis rates depending on specific interactions between the surfactants and reactant species, micellar aggregation number, CMC values, the extent of incorporation of reactants as counter ions in micelles etc [6,7]. Not only surfactants, but also cyclodextrins, by virtue of their cage like structure, may also influence the rate of hydrolysis reactions [8]. Cyclodextrins (CDs) are cyclic oligomers of α-D-glucose linked by α-1,4 glycoside bonds. Natural cyclodextrins are classified

as α-, β- or γ- CD according to whether they have 6, 7 or 8 α- D-glucopyranose residues respectively [9]. CDs can form inclusion complexes by means of non-covalent interactions, including van der Waals, hydrophobic, electrostatic, hydrogen bonding, steric effects etc with the molecules that fit into their cavities [10,11]. Because of their ability to form inclusion complexes, the reaction rates are generally reduced, i.e. CDs act here as stabilizers [12], but more interests are placed in the situation where CDs accelerate the reactions [13]. Moreover, surfactant-CD mixed systems draw a great interest in recent years due to their numerous applications in commercial formulations [14]. These systems can be used as a model for establishing the effect of cyclodextrins on phospholipids, an essential part of the cell membranes. The addition of cyclodextrin to a micellar solution leads to alter its physicochemical properties [15]. This is due the formation of CD-surfactant inclusion complexes where the stoichiometry (CD:surfactant) for majority of such cases are found to be of 1:1 or 1:2 or even 2:1 depending on the type of surfactant, tail chain length and also the size of the CD cavity [16].

A number of studies have already been reported separately on the basic hydrolysis of triphenylmethane dyes in the presence of cationic [17], anionic [18] and non-ionic [19] surfactants, cyclodextrins [20] and their mixed systems [21]. Nevertheless, only a little attention has been paid so far in determining the optimal operating environment for efficient removal of the dyes from wastewater using hydrolysis process. According to the literature, anionic surfactants greatly retard the rate of alkaline hydrolysis reaction of triphenylmethane dyes [18]. On the contrary, cationic surfactants generally accelerate the rate and their accelerating effect is much pronounced than the non-ionic surfactants [19].Thus in our present study, we have used three cationic surfactants (DTAB, TTAB, CTAB) of different chain lengths to monitor their effect on the hydrolysis rate. Again, in the presence of CDs, the probable mechanistic pathway of

their interaction to MG in alkaline medium and their efficiency to degrade the dye are yet to be known. Thus three CDs (α-, β-, γ-) of different cavity size have been used herein due to their ability to interact with MG and thereby influence the reaction rate. Besides, the insertion mechanism of MG inside the CD nanocavity has been carefully studied employing steady-state absorption technique and molecular docking analysis for better understanding of experimental findings. Thus, the present study may help us in finding out a system with optimally balanced combination of surfactant and CD to degrade malachite green at much faster rate. The reaction of malachite green in presence of alkali is a one-step reaction [22] and follows the pseudo-first order kinetics. All the experimental results have been discussed with proper correlation to the literature reports.

2. Materials and Methods

2.1. Materials

Malachite green (MG) has been procured from Merck, India as a chloride salt, $[C_6H_5C(C_6H_4N(CH_3)_2)_2]Cl$ and used as received. The surfactants dodecyltrimethylammonium bromide (DTAB), tetradecyltrimethylammonium bromide (TTAB), cetyltrimethylammonium bromide (CTAB) or in general alkyltrimethylammonium bromide (ATAB) as well as α, β and γ-cyclodextrins (CDs) have been purchased in the highest available purity from TCI, Japan. All other organic solvents used in this study have been obtained from Merck, India. Highly purified water from Milli-Q Ultra has been used for all sample preparation and dilution.

2.2. Methods

2.2.1. Experimental

Fresh solution of malachite green (MG) has usually been prepared for day to day work and used only after checking its concentration using the molar extinction coefficient, ε_{616} (MG) = 1.48 × 10^5 M^{-1} cm^{-1} [23]. The absorption spectra and kinetic measurements have been carried out using Shimadzu, UV-1800 Spectrophotometer equipped with a Peltier temperature controller, TCC-240A, maintaining a constant temperature of 298 K (± 0.1 K). The kinetics of the alkaline hydrolysis has been followed by measuring the decay in the absorbance at 616 nm as a function of time. The representative spectral change for the hydrolysis reaction has been shown in Fig. S1 ('S' stands for Supporting Material). The hydrolysis process has been pursued under pseudo-first order reaction conditions using NaOH concentration in large excess. The hydrolysis of MG has usually been followed up to 7-8 half-lives. In all the kinetic runs, the final concentration of MG has been kept at 1.25 × 10^{-5} M and the ionic strength (μ) of the medium has been maintained at 5.0 mM by adding KNO_3 solution. The observed first order rate constants (k_{obs}) and their standard deviations have been obtained by fitting to first order exponential decay of absorbance (A_t) *versus* time (t) plot using Microcal Origin 8.0.

2.2.2. Theoretical Methodology

The crystal structures of α-, β- and γ-CDs have been obtained from protein complexes (pdb id: 2ZYM, 2Y4S and 2ZYK for α-, β- and γ- CD respectively) available in Protein Data Bank (PDB). The CDs have been then extracted and added all the hydrogen and Gasteiger charges to prepare them for docking. The ground state geometry of malachite green (MG) has been optimized employing density functional theory (DFT) in conjugation with B3LYP functional and 6-31G* basis set in Gaussian 09 program suit [24]. The PDB structure of MG has been derived

from the optimized structure. MG has been considered as a ligand and CD as a receptor for docking studies. The molecular docking has been carried out applying the Lamarckian Genetic Algorithm (LGA), inculcated in the docking program Auto Dock 4.2 [25]. The CDs have been laid over a three dimensional grid box (126 x 126 x 126) $Å^3$ with 0.375 Å spacing. The output from Auto Dock has been analyzed using PyMOL software [26].

3. Results and Discussion

3.1 Kinetic Study

3.1.1 Hydrolysis of Malachite Green in Aqueous Medium

Hydrolysis causes the disruption of the extensive conjugation present in malachite green and thereby results in gradual diminution of the colour intensity. The hydrolysis reaction starts with the attack of the nucleophile, ^{-}OH to the carbocation center and results in the formation of a neutral carbinol base. The well-known mechanism of the reaction in aqueous phase [27] is shown in Scheme 1. Overall order of the reaction is found to be second i.e. first order in each of the reactant species, $[MG]_0$ and $[^{-}OH]_0$.

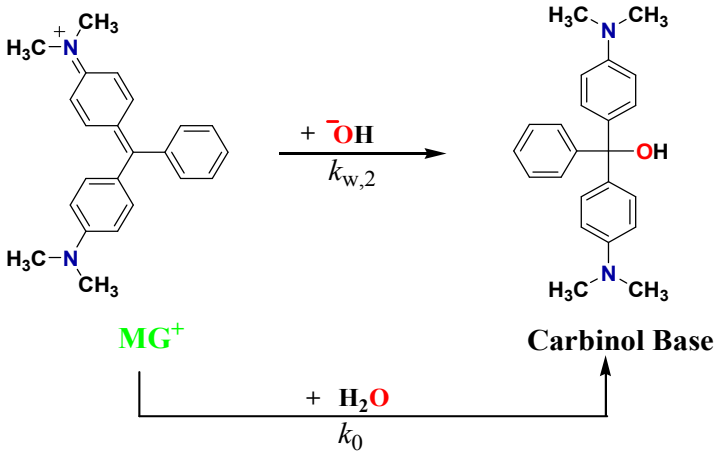

Scheme 1: Alkaline Hydrolysis of Malachite Green (MG)

The observed rate law can be expressed by Eq.1

$$\text{rate} = -\frac{\text{d[MG]}}{\text{dt}} = \{k_0 + k_{\text{w},2}[^{-}\text{OH}]_0\}[\text{MG}]_0 \quad (1)$$

Since, $[^{-}\text{OH}]_0 >> [\text{MG}]_0$

Therefore,

$$-\frac{\text{d[MG]}}{\text{dt}} = k_{\text{obs}}[\text{MG}]_0$$

$$\text{where}, k_{\text{obs}} = k_0 + k_{\text{w},2}[^{-}\text{OH}]_0 \quad (2)$$

where, $k_{\text{w},2}$ is second-order rate constant for the alkaline hydrolysis reaction. The value of $k_{\text{w},2}$ determined from the slope of the plot k_{obs} *versus* $[^{-}\text{OH}]_0$ (by Eq.2) is 2.508 (± 0.05) M^{-1} s^{-1}. The rate constant for hydrolysis of MG in pure water (k_0) obtained from the intercept of the plot is found to be of 9.75×10^{-5} s^{-1}.

3.1.2 Hydrolysis of Malachite green in Micellar Media

The influence of concentration of cationic amphiphiles (ATABs) on the rate of alkaline hydrolysis of malachite green (MG) has been examined in a wide interval that includes both the regions prior to the CMC and the regions after the CMC. (Fig.1). The Fig.1 shows that, k_{obs} increases only slightly on increasing the surfactant concentration until the CMC. This is an indication of weak pre micellar activity [19]. But afterwards, a sharp increase in k_{obs} can be observed due to the presence of micellar aggregates, and reaches to a limiting value, beyond which k_{obs} start to decrease considerably. The CMC values have been obtained kinetically by the minimum surfactant concentration required inducing a substantial change in the observed rate constant and found to be 11.3, 1.5 and 0.5 mM for DTAB, TTAB and CTAB respectively. These data show fair agreement with the literature values [28]. However, the CMCs derived kinetically

are found to be lower than those shown by the micellar systems of pure surfactants. This reduction has been ascribed to the known effect of electrolyte on CMC.

The alkaline hydrolysis of MG in cationic micellar media experiences micellar surface catalysis. The increment of surfactant concentration beyond its CMC leads to an increase of number of the micelles in the bulk phase [29], which in turn increases the concentration of micelle bound MG and $^{-}$OH in micellar Stern region. The MG is believed to be incorporated into the micelles by hydrophobic interaction for its existence of phenyl moieties and $^{-}$OH is gathered by the effect of coulombic attraction. This observation is in accordance with our earlier findings [30]. However, the phenomenon of ion-exchange at the micellar interface plays a vital role in determining the limiting value of k_{obs}. The gradual addition of surfactant results in increasing the concentration of counterion, Br^{-} in the medium. These are nonreactive counterions. Hence, a competition between Br^{-} and $^{-}$OH in the Stern region eventually inhibits the reaction rate [31].

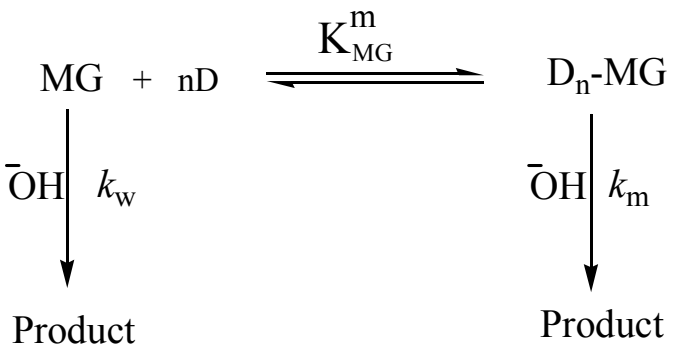

Scheme 2: Hydrolysis of MG in micellar solution

The experimental results can be interpreted quantitatively on the basis of Pseudo-phase Ion Exchange (PIE) model [32]. This model uses the micellar pseudo-phase formalism (Scheme 2) coupled with the assumption of ion-exchange at ionic micellar surface [33] and yields Eq. 3.

$$k_{obs} = \frac{k_{w,2}[^{-}OH]_T + (K^m_{MG}k_m - k_{w,2})m_{OH}[D_n]}{1 + K^m_{MG}[D_n]} \quad (3)$$

where $k_{w,2}$ & k_m are the rate constants in aqueous and micellar pseudo-phases respectively. K^m_{MG} is the association constant between MG and the micelles. D_n represents the micellized surfactant ($[D_n] = [ATAB]_T - CMC$). The m_{OH} is meant by $[^{-}OH]_m/ [D_n]$ ratio, where $^{-}OH_m$ is the hydroxyl ion at the micellar surface. The values of m_{OH} at different $[D_n]$ and at a constant $[^{-}OH]_T$ have been calculated by Eq. 4

$$m^2_{OH} + m_{OH}\left[\frac{[^{-}OH]_T + K^{OH}_{Br}[Br^{-}]_T}{(K^{OH}_{Br} - 1)[D_n]} - \beta\right] - \frac{\beta[^{-}OH]_T}{(K^{OH}_{Br} - 1)[D_n]} = 0 \quad (4)$$

where β is the fraction of surfactant head groups neutralised by counterions (β = 0.8) [34]. In order to resolve Eq. 4, the value of K^{OH}_{Br} = 15 have been used as it gives the best fit of the theoretical line. Moreover, the value of K^{OH}_{Br} for the most widely studied systems containing hydroxide ion and the micelle of bromide ion fall within the range of 10 − 20 [35]. The calculated values of m_{OH} is then used in Eq. 3 to evaluate k_m, K^m_{MG} and least squares, $\sum d_i^2$ (where, $d_i = k_{obs,i} - k_{cal,i}$ with $k_{obs,i}$ and $k_{cal,i}$ representing the observed and calculated rate constant values at i^{th} concentration of micellized surfactant, $[D_n]_i$) values using non-linear least-square technique. The value of k_w (first-order rate constant in aqueous phase) is kept constant and identical to the value previously obtained in aqueous phase. The values of k_m and K^m_{MG} so obtained from Eq. 3 for different micellar systems have been presented in Table 1 along with the

calculated values of the rate constants, k_{cal}, at K_{Br}^{OH} = 15. The satisfactory fit of observed data to Eq. 3 is evident from the plot of Fig. 1, where the solid line has been drawn by the calculated data points (k_{cal}) for different micellar systems employing the value of K_{Br}^{OH} = 15.

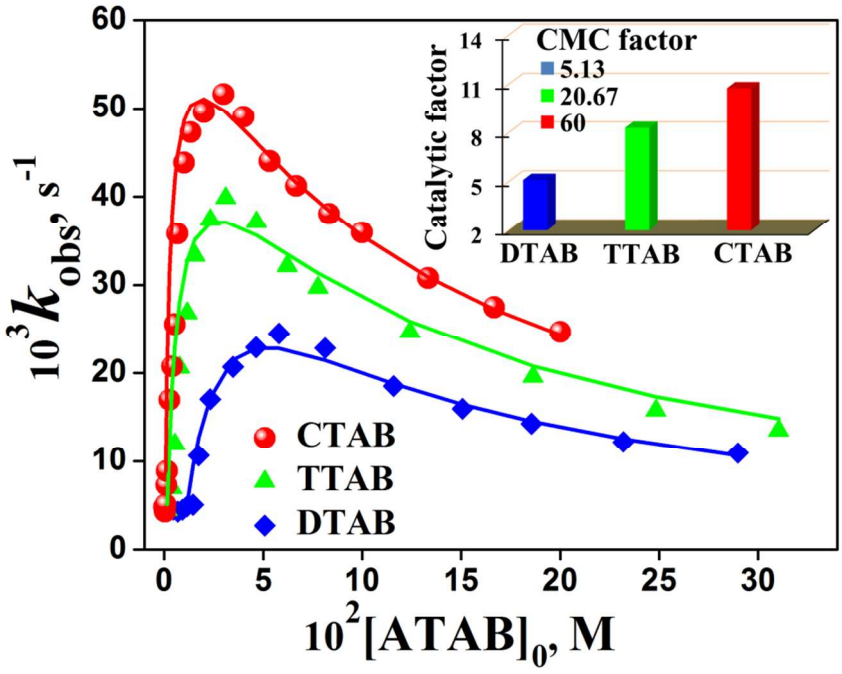

Fig. 1 Plots of k_{obs} *versus* concentration of surfactants of different chain lengths for alkaline hydrolysis of MG at 298 K. $[MG]_0 = 1.25 \times 10^{-5}$ M, $[^-OH]_0 = 1.875$ mM.
Inset: Catalytic factor (k_{obs}^{max}/k_w) in different micellar systems.

The lower values of K_{MG}^{m} for CTAB micelles compared to DTAB may be attributed to the fact that the longer hydrocarbon chain of CTAB may result in folding and thus provide less space for binding to MG [36]. Hence, the highest value of k_m in CTAB micellar medium (Table 1) helps us to recognize the concurrent effect on hydrolysis reaction caused by the increment of local concentration of the reactant species at the micellar surfaces and the lowering of polarity at the micellar pseudo-phase compared to the bulk aqueous phase [19]. The effect of polarity on the hydrolysis rate is well understood by Hughs and Ingold rule that is the rate of the formation of a

neutral product from two oppositely charged reactants gets accelerated as the polarity of the medium decreases [37]. The rate acceleration caused by lowering of polarity in the micellar Stern region has been discussed in our previous work too [30]. Moreover, CTAB being the highest homologue among ATABs possesses the lowest value of CMC. Therefore, the concentration of the nonreactive counterion, Br^- in equilibrium with the CTAB micellar system is also much less when the micellization process begins. Thus, CTAB shows the maximum catalytic effect on the hydrolysis rate among the ATABs.

The characteristic behaviour of catalysis exhibited by all the cationic micelles (Fig. 1) allows us to compare quantitatively the catalytic influence of the surfactants on the rate of alkaline hydrolysis of malachite green. The catalytic effect is found to increase towards the higher homologue of ATABs *i.e.*, it follows the order: DTAB ($-C_{12}$) < TTAB ($-C_{14}$) < CTAB ($-C_{16}$). The maximum degree of catalytic activity in different micellar systems has been shown in Fig. 1 Inset introducing the parameter, catalytic factor (k_{obs}^{max}/k_w), and for each value of k_{obs}^{max}/k_w, the corresponding concentration of surfactant has been presented in terms of CMC factor ([ATAB] for k_{obs}^{max} to CMC ratios). As can be seen from Fig. 1 & Inset, the catalytic effect exerted by CTAB micellar system reaches to the maximum degree at [CTAB] of 30.0 mM which is nearly 60 times its CMC under the condition of our present study. While TTAB and DTAB exhibit their maximum catalytic activity at concentrations correspond to 20 times and 5 times to their respective CMC values.

Table 1 Kinetic parameters for alkaline hydrolysis of MG in presence of surfactants at 298 K[a]

DTAB			TTAB			CTAB		
10^3[DTAB]$_0$, M	$10^3 k_{obs}$, s^{-1}	$10^3 k_{cal}$,[b] s^{-1}	10^3[TTAB]$_0$, M	$10^3 k_{obs}$, s^{-1}	$10^3 k_{cal}$, s^{-1}	10^3[CTAB], M	$10^3 k_{obs}$, s^{-1}	$10^3 k_{cal}$, s^{-1}
0.0	4.80	—	0.0	4.81	—	0.0	4.80	—
11.6	4.89 ± 0.1[c]	5.20	1.6	4.44 ± 0.1	5.11	0.67	5.1 ± 0.1	8.81
14.5	5.07 ± 0.1	9.43	3.9	6.95 ± 0.1	18.13	1.00	7.3 ± 0.1	14.99
17.4	10.66 ± 0.2	12.69	7.8	20.64 ± 0.3	28.06	2.67	17.0 ± 0.2	31.48
23.2	17.07 ± 0.3	17.19	11.7	26.84 ± 0.2	32.72	4.0	20.8 ± 0.4	37.92
34.8	20.72 ± 0.3	21.50	15.5	33.29 ± 0.5	35.13	6.67	35.8 ± 0.8	44.79
46.4	22.93 ± 0.5	22.81	23.3	37.33 ± 0.7	36.99	10.0	43.9 ± 1.1	48.67
58.0	24.52 ± 0.3	22.83	31.1	39.84 ± 0.6	37.11	20.0	49.6 ± 1.3	51.09
81.2	22.86 ± 0.6	21.48	46.6	37.10 ± 0.4	35.61	30.0	51.7 ± 0.8	49.76
116.0	18.56 ± 0.5	18.82	77.6	29.73 ± 0.3	31.34	40.0	49.1 ± 1.0	47.61
150.8	15.99 ± 0.4	16.45	124.2	24.71 ± 0.4	25.88	66.7	41.2 ± 0.7	41.64
185.6	14.31 ± 0.1	14.53	186.3	19.62 ± 0.2	20.81	100.0	35.9 ± 0.8	35.54
232.0	12.23 ± 0.2	12.52	248.4	15.81 ± 0.2	17.35	133.3	30.8 ± 0.9	30.88
290.0	10.92 ± 0.3	10.65	310.5	13.49 ± 0.1	14.86	200.0	24.7 ± 0.5	24.39
$10^6 \sum d_i^2$		0.098			0.447			13.849
k_m, s^{-1}		9.7 ± 0.5			15.1 ± 0.6			18.3 ± 0.9
K_{MG}^{m}, M^{-1}		21.5 ± 0.3			9.1 ± 0.4			9.3 ± 0.4

[a] $[^-OH]_0$ = 1.875 mM. [b]Calculated from Eq. 3 & 4 with β = 0.8, K_{Br}^{OH} = 15, $k_{w,2}$ = 2.508 M^{-1} s^{-1}. [c]Error limits are standard deviations.

3.1.3. Influence of α-, β- and γ- Cyclodextrins on the Reaction Rate

The influence of cyclodextrins (CDs) on the rate of alkaline hydrolysis of MG is shown in Fig. 2. As can be observed, all the CDs catalyze the hydrolysis reaction, but in different extents. The maximum catalytic influence of the CDs has been presented in Fig. 2 Inset in terms of catalytic factor (k_{obs}^{max}/k_w) at a common fixed CD concentration (1.0 mM). The experimental behaviour can be explained by taking into consideration the mechanistic behaviour as shown in Scheme 3

where CD-catalyzed and hydrolytic reaction take place through MG-CD inclusion complex and in the bulk aqueous phase respectively. The catalytic effect exerted by CD can be attributed to the nucleophilic attack by the ionized secondary hydroxyl group of CD on the MG associated with CD [38]. Therefore, it must be assumed that the geometry of the inclusion complex formed by the CDs of different cavity size is influential here for the rate variations found in Fig. 2.

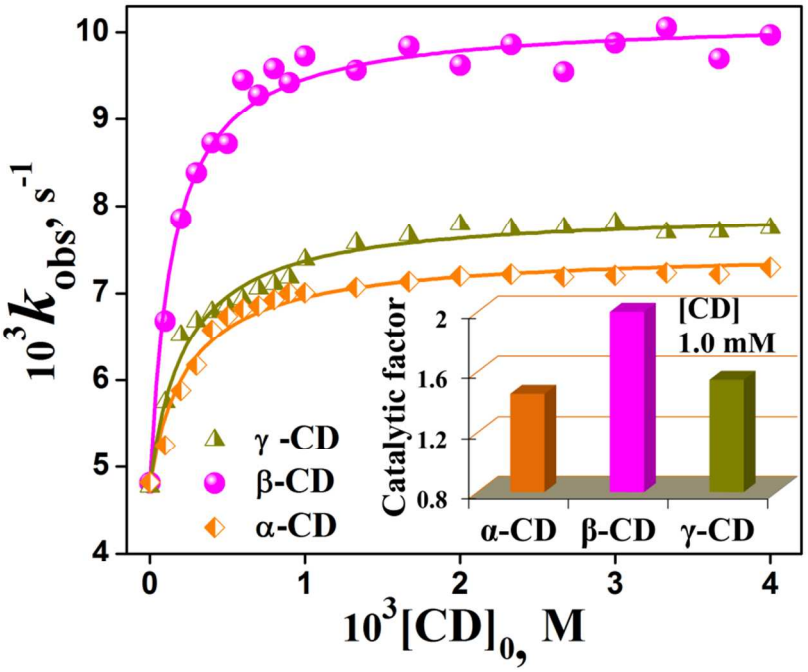

Fig. 2 Plots of k_{obs} *versus* $[CD]_0$ for the reaction of MG and ^-OH in the aqueous medium at 298 K. $[MG]_0 = 1.25 \times 10^{-5}$ M, $[^-OH]_0 = 1.875$ mM.

Inset: Catalytic factor (k_{obs}^{max}/k_w) in different cyclodextrin systems at fixed [CD] = 1.0 mM.

In the presence of CD, binding of MG inside the host (CD) cavity gives the reaction intramolecular character which enhances the rate of the reaction. This concept is quite similar to enzyme-like catalysis [39]. The supramolecular hosts bind MG in such a way that the electrophilic centre of the carbocationic dye is positioned close to the deprotonated secondary

hydroxyl groups of CD. The proximity of the two groups in different MG-CD inclusion complexes will determine the efficiency of catalytic behaviour of the respective CDs [40].

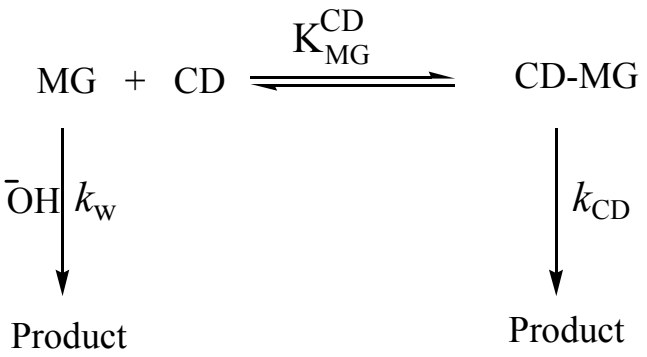

Scheme 3: Hydrolysis of MG in aqueous solution of CD

According to the Scheme 3, for a substrate that experiences an uncatalyzed reaction in a given medium as well as a catalyzed reaction by the formation of 1:1 substrate–CD complex, the expected variation of k_{obs} with CD concentrations can be given by Eq. 5 [38].

$$k_{obs} = \frac{k_w + k_{CD}\, K_{MG}^{CD}\, [CD]_0}{1 + K_{MG}^{CD}\, [CD]_0} \qquad (5)$$

K_{MG}^{CD} is the equilibrium binding constant of MG to the cyclodextrin, and k_{CD} is the pseudo-first order rate constant for the CD-catalyzed reaction. The value of k_w is kept constant and identical to the value previously obtained in aqueous phase. The K_{MG}^{CD} and k_{CD} values are obtained by fitting the experimental data to Eq. 5 by a non-linear regression analysis and presented in Table 2. The k_{CD} values indicate that the rate acceleration by CDs follows the order: β-CD > γ-CD > α-CD i.e., β-CD catalyzes the reaction to the most extent among the CDs.

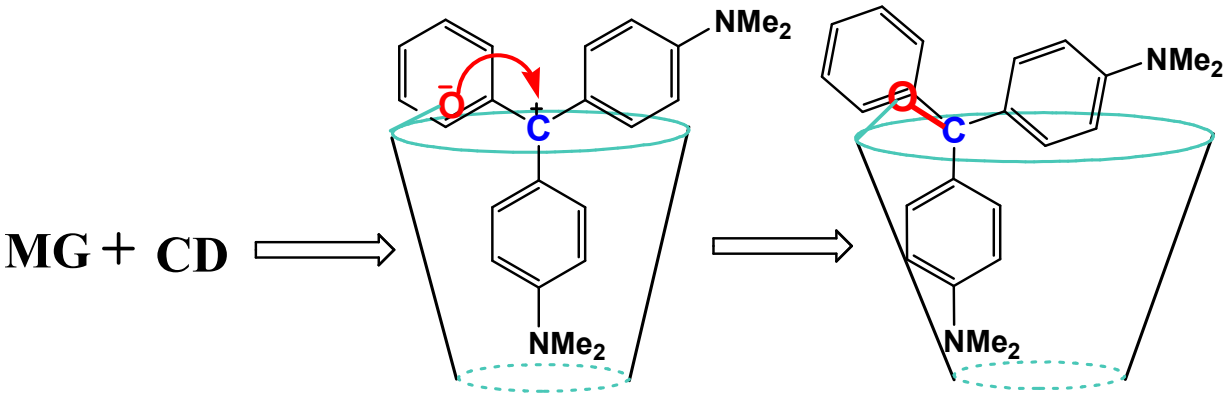

Scheme 4: Mechanism of hydrolysis reaction in CD medium

The mechanism of the CD-catalyzed process has been shown in Scheme 4, where cyclodextrin as its oxyanion reacts with carbocationic dye (MG) resulting a tetrahedral complex. Thus we have to consider not only the closest approach of the two reacting centers, but also the geometric change of the MG-CD complex needed for the entire reaction for a suitable orientation of the tetrahedral complex so formed [41]. A detailed conformational search regarding different geometrical orientations of MG inside the various CD cavities have been undertaken in the following sections *viz*. 4.1 & 4.2 based on steady-state absorption and molecular docking studies respectively in order to ascertain the observed rate variation in different CD systems.

Table 2 Kinetic parameters for alkaline hydrolysis of MG in presence of CDs at 298 K[a].

$10^3[CD]_0$, M	α-CD		β-CD		γ-CD	
	10^3K_{obs}, s^{-1}	10^3k_{cal}[b], s^{-1}	10^3K_{obs}, s^{-1}	10^3k_{cal}, s^{-1}	10^3K_{obs}, s^{-1}	10^3k_{cal}, s^{-1}
0.0	4.82	4.80	4.81	4.80	4.77	4.80
0.20	5.88 ± 0.04[c]	5.96	7.85 ± 0.05	7.89	6.52 ± 0.08	6.29
0.40	6.58 ± 0.06	6.41	8.73 ± 0.10	8.73	6.79 ± 0.07	6.84
0.60	6.82 ± 0.02	6.64	9.46 ± 0.11	9.12	6.94 ± 0.09	7.12
0.80	6.93 ± 0.08	6.79	9.59 ± 0.08	9.35	7.11 ± 0.08	7.29
1.00	7.01 ± 0.04	6.89	9.73 ± 0.04	9.50	7.38 ± 0.08	7.40
1.33	7.07 ± 0.10	6.99	9.57 ± 0.07	9.66	7.57 ± 0.4	7.53
2.00	7.19 ± 0.05	7.11	9.62 ± 0.07	9.83	7.79 ± 0.05	7.67
2.33	7.22 ± 0.05	7.15	9.86 ± 0.04	9.87	7.74 ± 0.03	7.71
3.00	7.21 ± 0.3	7.20	9.88 ± 0.06	9.94	7.81 ± 0.7	7.77
3.33	7.23 ± 0.03	7.22	10.06 ± 0.03	9.97	7.69 ± 0.5	7.79
4.00	7.29 ± 0.04	7.25	9.97 ± 0.04	10.01	7.74 ± 0.04	7.83
$10^6\sum d_i^2$		0.308		0.652		0.244
10^3k_{CD}, s^{-1}		7.4 ± 0.10		10.3 ± 0.11		8.0 ± 0.08
K_{MG}^{CD}, M^{-1}		4050 ± 90		6700 ± 110		4370 ± 80

[a] $[^-OH]_0$ = 1.875 mM. [b] Calculated from Eq. 5, $k_w = 4.8 \times 10^{-3}$ s^{-1}. [c] Error limits are standard deviations.

Thus, Table 1 clearly reveals that the alkaline hydrolysis reaction is catalyzed to the highest extent in presence of CTAB micellar medium among the ATABs. Similarly, β-CD accelerates the reaction most efficiently among the CDs (Table 2). Therefore, a kinetic study of the influence of surfactant concentration on the hydrolysis reaction at a fixed [CD] would provide a guidance to reach to an optimal condition for the fastest degradation of MG. In this context, only β-CD has been chosen as a component of the surfactant-CD mixed system for its better catalytic activity than α- or γ-CD.

3.1.4 Influence of ATAB – β-CD Mixed Systems on the Reaction Rate

The influence of surfactant concentration on k_{obs} for alkaline hydrolysis of MG in the presence of a constant concentration of β-CD, $[\beta\text{-CD}]_0$ = 1.0 mM has been shown in Fig. 3. As we increase the surfactant concentration, k_{obs} initially decrease until it reaches to a minimum value. This fact is attributed to the complexation of surfactant monomer with β-CD displacing MG to the bulk phase. The CD catalytic route thereby gets lost and consequent reduction of the rate is observed. Dorrego and coworkers reported a similar observation with the base hydrolysis of m-nitrophenylacetate in mixed systems made up of alkyltrimethylammonium micelles and α- or β-cyclodextrins [28]. After the minima of the curve k_{obs} *versus* [ATAB], k_{obs} exhibits the same kind of [ATAB] dependence as we have observed in the absence of CD, that is it increases rapidly upto a limiting value and falling gradually thereafter. The concentration of surfactant at that minimum value of k_{obs} has been taken as the onset of micellization and found to be 17.5, 3.6 and 1.5 mM for DTAB, TTAB and CTAB respectively. The CMCs have been found to be displaced to higher values than that of the respective surfactants in absence of CD. This fact is ascribed solely to the complexation of surfactant monomers with β-CD [16]. At [ATAB] > CMC, the observed catalytic effect is due to the micellar catalysis by ATAB micelles and it is similar to what we have found in section 3.1.2. The catalytic efficiency of the mixed systems can be identified by the catalytic factor, *i.e*. the ratio of the observed rate constant at the maximum, k_{obs}^{max}, and that at micellization concentration, k_{obs}^{min}. The catalytic factor, $k_{obs}^{max}/k_{obs}^{min}$, of the various mixed systems has been found to be 7.5, 7.58 and 7.72 for DTAB, TTAB and CTAB respectively. The value of $k_{obs}^{max}/k_{obs}^{min}$ is quite independent on the nature of the surfactants. This result contrasts with the values of $k_{obs}^{max}/k_w = 5.11$, 8.51 and 11.39 for the same surfactants in pure micellar systems. This loss of catalytic efficiency of the surfactants in the mixed systems is

due to the complexation between surfactant monomer and β-CD. This is because; the complexation displaces the CMC to higher values, which in turn increases the concentration of non-reactive counterions (Br^-) at the point of micellization. Moreover, the percentage of uncomplexed β-CD in equilibrium with the micellar systems increases together with the length of the hydrocarbon chain of the surfactants [28]. The increase in concentration of uncomplexed β-CD causes in shifting the minimums of the curves k_{obs} *versus* [ATAB] to higher value of k_{obs} as the chain length of the surfactants increases. Both of the above incidents reduce the value of $k_{obs}^{max} / k_{obs}^{min}$.

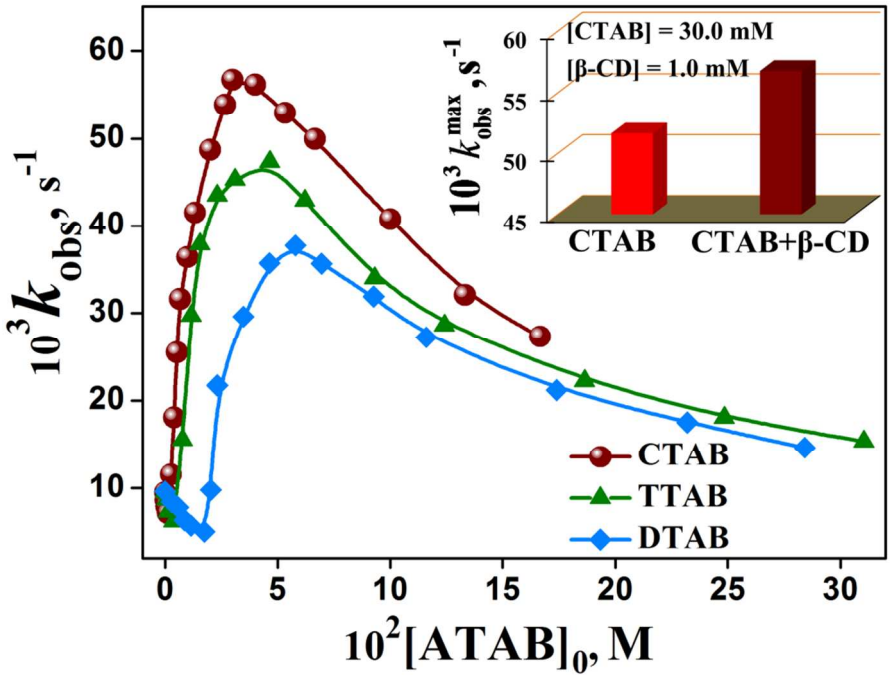

Fig. 3 Influence of ATAB concentration on k_{obs} for alkaline hydrolysis of MG in the presence of β-CD. $[β\text{-CD}]_0$ = 1.0 mM, $[^-OH]_0$ = 1.875 mM, T = 298 K

Inset: Maximum rate constant, k_{obs}^{max}, in CTAB−β-CD mixed and CTAB micellar systems.

As we are concerned about the fastest degradation of malachite green, that is the value of the maximum rate constant, k_{obs}^{max}, then it can undoubtedly call for CTAB−β-CD mixed system to be the most efficient environment in this scenario (Fig. 3 Inset). Fig 3 Inset shows a comparison of k_{obs}^{max} value between CTAB−β-CD mixed and CTAB micellar systems and it is observed that k_{obs}^{max} acquires higher value in CTAB−β-CD mixed system than in pure CTAB micellar system. Hence, the desired optimum condition for the most effective degradation of malachite green is found to be as $[CTAB]_0$ = 30 mM at $[\beta\text{-CD}]_0$ = 1.0 mM.

4. Characterization of MG–CD inclusion complex

4. 1. Absorption studies

The change in absorption spectra of MG upon the quantitative addition of CD implies a significant interaction between them. Fig. S2 shows that the absorbance of MG at 616 nm decreases gradually with CD concentration. The stoichiometry of binding between MG and CDs has been ascertained using Benesi-Hildebrand (B-H) equation (Eq. 6) [42]:

$$\frac{1}{\Delta A} = \frac{1}{A' - A^0} + \frac{1}{K(A' - A^0)[CD]_0} \quad (6)$$

where, A^0 is the initial absorbance of the free guest (MG), ΔA is the change in absorbance of the inclusion complex (MG–CD), A' is the absorbance at the highest concentration of CD. The experimental results show a linear plot for $1/(\Delta A)$ *versus* $1/[CD]_0$ throughout the entire concentration range of all the CDs. This clearly indicates the 1:1 MG−CD complexation [43]. Fig. 4 shows the B-H plots for MG–β-CD, MG–α-CD and MG–γ-CD inclusion complexes. The

association constant (K) of the host-guest inclusion complexes have been evaluated from the intercept and slope of these plots, and found as 4.89 (± 0.07) × 10^2, 21.04 (± 0.04) × 10^2 and 5.42 (± 0.03) × 10^2 M^{-1} for α-CD, β-CD and γ-CD respectively.

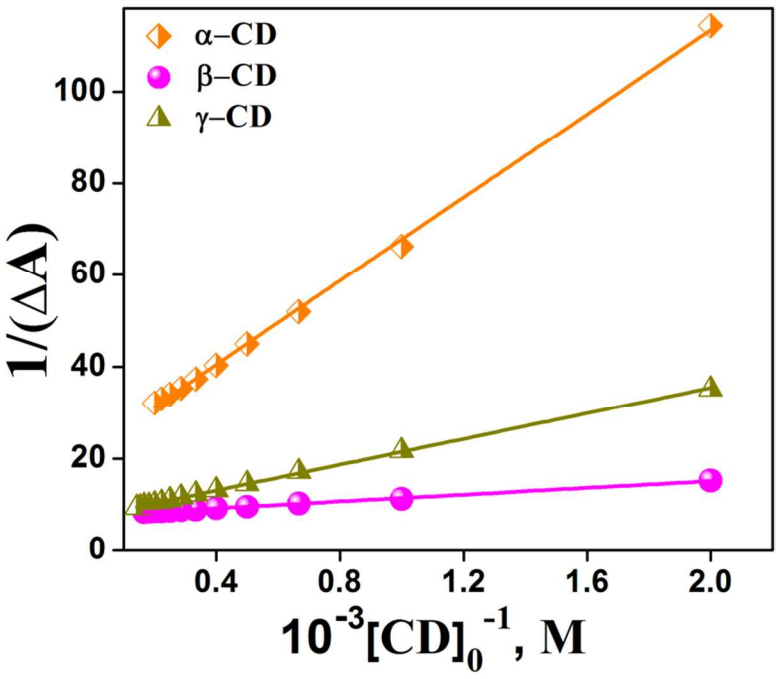

Fig. 4 Benesi-Hildebrand plot for the 1:1 MG– CD inclusion complex in aqueous media.

The above results indicate that MG links to only one CD molecule. To substantiate the discussion, the molecular dimensions of MG have been calculated theoretically using the DFT method (Scheme 5) with B3LYP functional and 6-31G* basis set, and data indicates that the complete incorporation of MG inside any of the CD cavity is not possible. It is well reported that CD molecules acquire truncated, right-cylindrical, cone-shaped structure with a height of 7.8 Å and a central cavity with diameters of the narrower and wider rim of α-, β- and γ-CD are 4.5–5.7 Å, 6.2–7.8 Å and 7.9–9.5 Å respectively [44,45].

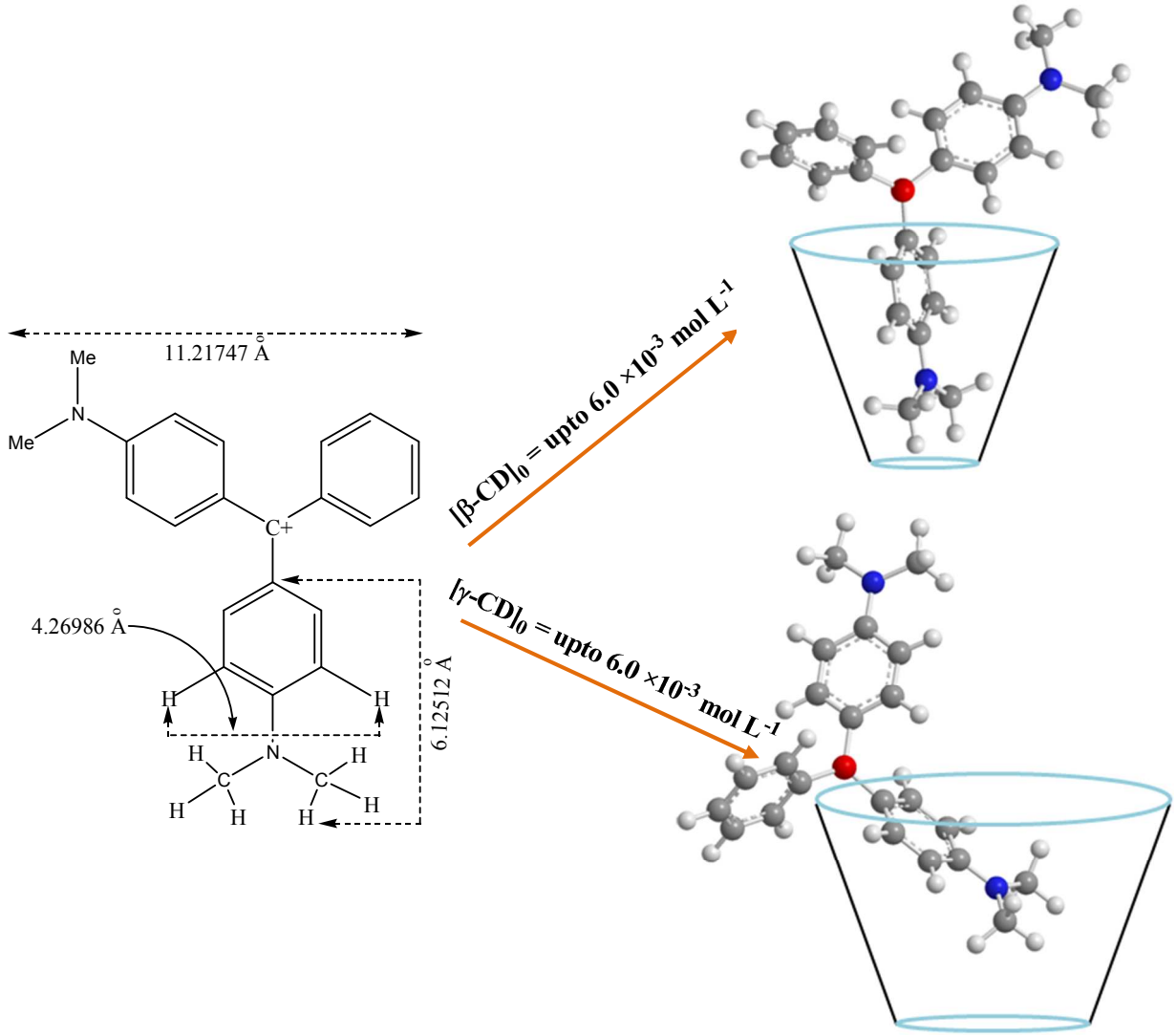

Scheme 5: Inclusion of MG inside the CD cavity

Keeping in mind the spatial distribution of the three phenyl rings and the size of MG (height and width), it is clear that only a part of MG can enter inside the CD cavity as shown in Scheme 5. The length of each of the phenyl rings bearing the $–NMe_2$ (dimethylaminobenzene) group (6.12 Å) and that of the benzene moiety (3.97 Å) of MG are compatible with the height of CD cavity.

Thus, during the process of inclusion, it is possible for the dimethylaminobenzene part of MG to penetrate the CD cavity, keeping the benzene moiety exposed to the bulk water, or vice-versa. If MG orients in the latter pattern, there is no scope of the change in spectral behaviour, this is because in this situation the extended conjugated part of MG containing the auxochrome, $–NMe_2$, remains outside the CD cavity. Therefore, a considerable change in the absorption of MG can only be produced if the dimethylaminobenzene part insert inside the CD cavity.

The minute change in the absorption profile of MG–α-CD system indicates the weak interaction between α-CD and dimethylaminobenzene moiety (6.12 Å). It is presumably due to the dimensional incongruity, thereby producing the small value, 4.89 (± 0.07) × 10^2 M^{-1} of association constant (K) by MG–α-CD inclusion complex. However, the considerable diminution in absorbance of MG upon the quantitative addition of β-CD (up to 6 mM) is probably due to excellent dimensional compatibility between the dimethylaminobenzene moiety (6.12 Å) and the β-CD cavity (6.2–7.8 Å), indicating effective interaction between them (Scheme 5). This is reflected by the large value of K, 21.04 (± 0.04) × 10^2 M^{-1} for MG−β-CD inclusion complex. The significant change in the absorption profile of MG–γ-CD system clearly supports the inclusion of the dimethylaminobenzene part inside the γ-CD core. But the much larger γ-CD cavity (7.9–9.5 Å) compels us to predict the two types of inclusion complexes, where the dimethylaminobenzene moiety (6.12 Å) may enter inside the γ-CD core either alone or together with the benzene moiety (3.97 Å). It is evident that both forms of the MG–γ-CD complex are capable of inducing a considerable change in the absorption behaviour of MG in γ-CD medium.

4. 2. Molecular Docking Studies:

Molecular docking is frequently being used to predict the orientation of a guest molecule relative to a receptor when bound to each other [46,47]. Molecular docking analysis is accomplished herein to predict the probable location of MG within the complex architecture of cyclodextrins. The convergence of the conformational search employing molecular docking model indicates the reliability of the experimental results for extracting structural orientations.

According to the docking model, relative orientation of MG inside the α-CD nanocavity (Fig. 5a) allows us to identify a vertical mode of insertion of the benzene moiety with a binding energy of -5.38 kcal mol^{-1}. Another docked conformation (not shown) with dimethylaminobenzene as the inserting moiety (-2.7 kcal mol^{-1}) is also found to form. It is evident that the later docked form is energetically less contributing to the MG–α-CD inclusion complex. Hence the minute change in the absorption behaviour of MG in α-CD medium is well justified by the later docked form (Fig. S2.a). In β-CD, dimethylaminobenzene moiety of MG inserts in somewhat tilted fashion producing a binding energy of -5.44 kcal mol^{-1} (Fig. 5b). The high negative binding energy with a torsional energy of 1.49 kcal mol^{-1} clearly reveals that MG snugly fits into the host cavity. The large diminution in absorbance of MG in presence of β-CD fairly supports the effective interaction between MG and β-CD (Fig. S2.b). However, the other docked form, albeit energetically less favourable (-4.98 kcal mol^{-1}), is also found to be formed by the benzene moiety as inserting group in the same tilted fashion (Fig. S3). In case of γ-CD, the large cavity volume of which (7.9–9.5 Å) indeed strongly prohibits the benzene moiety (3.97 Å) to insert alone inside the host. The docked conformations in Fig. 5c & d exhibit that MG orients itself in two most probable arrangements inside the γ-CD core. One exhibits a bent vertical insertion of dimethylaminobenzene moiety (Fig. 5c), and another shows the horizontal insertion of the same

together with the benzene moiety (Fig. 5d) inside the empty pocket of γ-CD. The considerable change in the absorption profile of MG–γ-CD system is justified once again by the two docked forms (Fig. S2.c). Between the two docked forms, the latter has a binding energy of -5.79 kcal mol^{-1}, seems more favourable to be formed than the first one (-4.99 kcal mol^{-1}) with the same torsional energy (1.49 kcal mol^{-1}). As we have stated previously that the proximity of attacking group (here, deprotonated secondary hydroxyl group of CD) to the electrophilic center of the carbocationic dye plays a vital role over the rate variation in different CD environments. The distance between carbocation center and the closest secondary hydroxyl is 5.268 Å in β-CD, but only 4.466 Å in α-CD (Fig. 5a & b). Therefore, nucleophilic attack by the ionized secondary hydroxyl group is seemed to be taken place with greater ease in MG-α-CD inclusion complex. But the lower catalytic effect produced by α-CD (Table 2) makes us to believe that the required geometric change of the product to a tetrahedral arrangement is difficult due to the small cavity size of α-CD and this fact outweighs the privilege acquired by the nearest approach of the two reacting centers. Whereas, in γ-CD, it is seen that the inserting groups of MG penetrates deeply inside the γ-CD core (Fig. 5c & d) producing a long distance between the two reacting centers (6.131 Å and 6.311 Å for Fig. 5c & d respectively). Therefore, the initial nucleophilic attack by the deprotonated secondary hydroxyl of γ-CD to the electrophilic center of the dye occurs only to a lesser extent. Hence, the order of catalytic effect of CDs as we find in kinetic studies (i.e., β-CD > γ-CD > α-CD) is well justified by the above absorption and molecular docking studies.

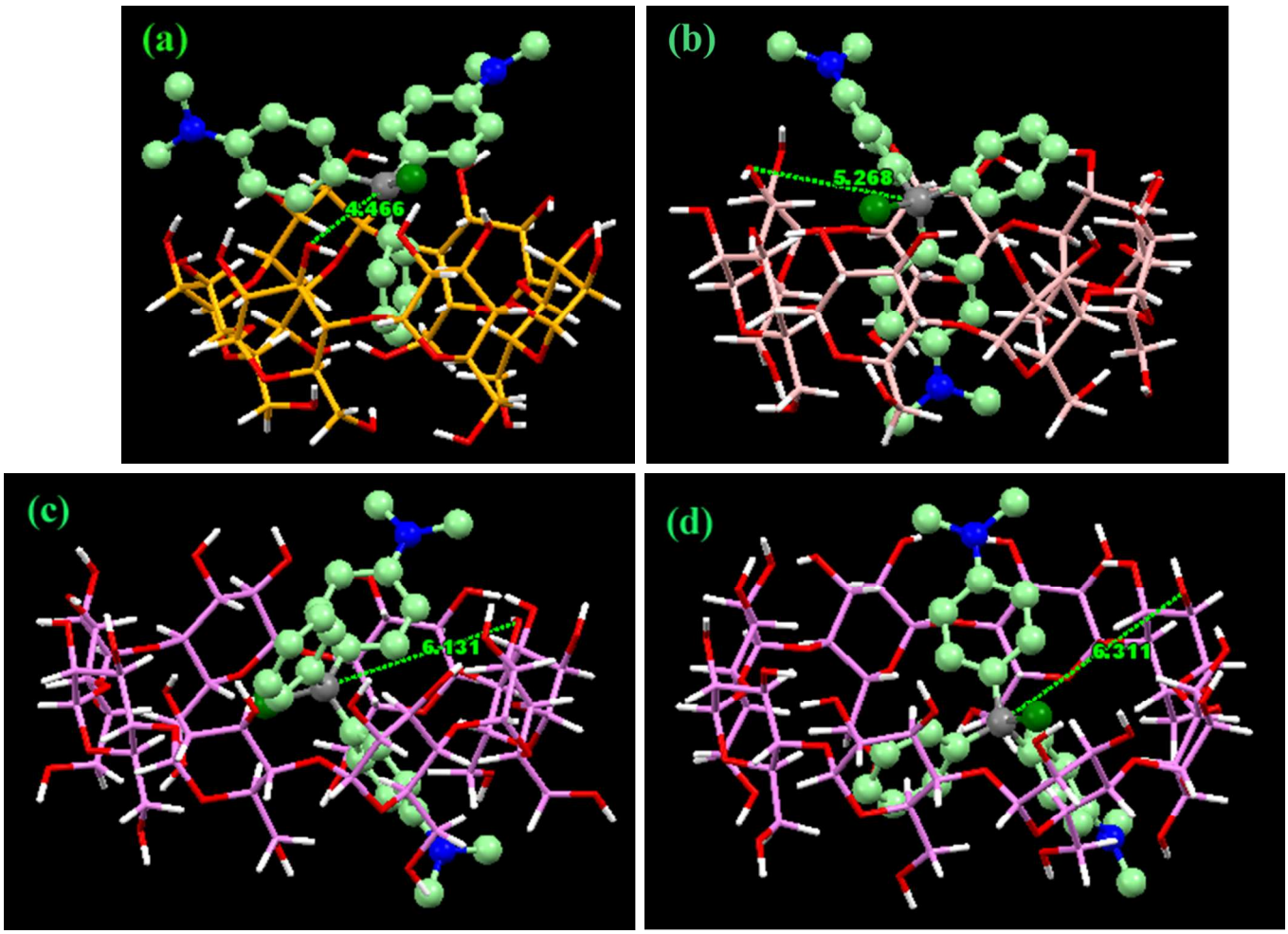

Fig. 5 Molecular docking of 1 : 1 complex for (a) MG-α-CD, (b) MG-β-CD, (c) MG-γ-CD (tilted) and (d) MG- γ-CD (horizontal). MG and CDs are depicted in the ball stick and capped stick model respectively (Distances given in the pictures are in Å units).

5. Conclusion

Our target was finding out an optimum condition in terms of surfactant and CD concentration at ambient pressure and temperature to degrade MG proficiently by alkaline hydrolysis process. In this context, among the C12, C14 and C16 variants of ATABs, the C16 homologue (CTAB)

shows its marked catalytic effect on the hydrolytic rate. Similarly, among α-, β- and γ-CDs, the β-CD having the proper cavity size exhibits effective interaction with MG and thereby facilitates appreciably the nucleophilic attack of its ionized secondary hydroxyl group to the carbocation center of MG. The rate variation by the CDs is manifested by the 1:1 host-guest inclusion complexes between MG and CDs. The relative orientations of MG inside the CD nanocavities are unveiled by steady-state absorption technique along with quantum mechanical calculations using density functional theory (DFT) and molecular docking analysis. All of these studies indicate that the geometric fit of MG within different CD cavities will determine the efficiency of catalytic activity of the respective CDs. The mixed system composed of CTAB and β-CD eventually serves the right purpose of this study exhibiting the maximum value of k_{obs} among all the ATAB– β-CD mixed systems. The condition for the fastest degradation of MG by alkaline hydrolysis process has been achieved at $[CTAB]_0$ = 30 mM in presence of $[\beta\text{-CD}]_0$ = 1.0 mM at normal temperature and pressure. Thus, the present study explicitly points towards an efficient route for decontaminating of malachite green from industrial wastewater in a comparatively greener way.

Acknowledgement

SD sincerely acknowledges University Grants Commission (UGC), New Delhi, for junior research fellowship and AK acknowledges the Council of Scientific and Industrial Research (CSIR), New Delhi, for senior research fellowship. TM gratefully acknowledges UGC, Govt. of India for funding with BSR-Startup grant (No.F.20-35/2013 (BSR) dated 09.12.2013) and DST PURSE program to University of Kalyani.

5. References

1. D. F. Duxbury, *Chem. Rev*., 1993, **93,** 381–433.
2. L. S. Andrade, L. A. M. Ruotolo, R. C. Rocha-Filho, N. Bocchi, S. R. Biaggio, J. Iniesta, V. Garcˇıa-Garcia and V. Montiel, *Chemosphere*, 2007, **66**, 2035–2043.
3. F. Robina, R. Faiza, B. Sofia, S. Maria, K. Sajjad, F. Umar, R. Abdur, F. Ather, P. Arshed, M. al Hassan and S. F. Shaukat, *World Appl. Sci. J*., 2009, **6**, 234–237.
4. F. Robina, L. F. Kai, S. F. Shaukat and J. J. Huang, *J. Environ. Sci*., 2003, **5**, 710–714.
5. W. R. Mabey and T. Mill, *J. Phys. Chem*., 1978, **7**, 383–415.
6. A. S. Al-Ayed, M. S. Ali, H. A. Al-Lohedan, A. M. Al-Sulaim and Z. A. Issa, *J Colloid Inter Sci.*, 2011,**361**, 205–211.
7. H. A. Al-Lohedan, *J Chem Soc, Perkin Trans*, 1995, **2**, 1707–1713.
8. O. S. Tee, *Ad*v. *Phys. Org. Chem.* 1994, **29**, 1–85.
9. V. T. D'Souza and K. B. Lipkowitz, *Chem. Re*v., 1998, **98**, 1741–1742.
10. K. A. Connors, *Chem. Rev.*, 1997, **97**, 1325–1357.
11. X. Zhang and C. Wang, *Chem. Soc. Rev.*, 2011, **40**, 94–101.
12. N. M. Rougier, D. L. Cruickshank, R. V. Vico, S. A. Bourne, M. R. Caira, E. I. Buján and R. H. de Rossi, *Carbohydr. Res.*, 2011, **346**, 322–327.
13. P. A. Prasantha, N. C. Sandhya, B. K. Kempegowda, D. G. Bhadregowda, K. Mantelingu, S. Ananda, K. K. S. Rangappa and M. N. Kumara, *J. Mol. Catal. A: Chem.* 2012, **353–354**, 111–116.
14. D. J. Jobe, V. C. Reinsborough and S. C. Wetmore, *Langmuir* 1995, **11**, 2476–2479.
15. H. Mwakibete, R. Cristantino, D. M. Bloor, W. Wyn-Jones and J. F. Holzwarth, *Langmuir* 1995, **11**, 57–60.

16. A. J. M. Valente and O. Söderman, *Adv. Colloid Interface Sci*., 2014, **205**, 156–176.
17. A. Raducan, A. Olteanu, M. Puiu and D. Oancea, *Cent. Eur. J. Chem*., 2008, **6**, 89–92.
18. Y. Zhang, X. Li, J. Liu and X. Zeng, *J. Disp. Sci. Tech*., 2002, **23**, 473–481.
19. B. Samiey and A. R. Toosi, *Bull. Korean Chem. Soc*., 2009, **30**, 2051–2056.
20. V. Raj, A. Sarathi, T Chandrakala, S. Dhanalakshmi, R. Sudha and K. Rajasekaran, *J. Chem. Sci.*, 2009, **121**, 529–534.
21. O. Soriyan, O. Owoyomi and A. Ogunniyi, *Acta Chim. Slov.*, 2008, **55**, 613–616.
22. C. D. Ritchie, D. J. Wright, D. S. Huang and A. A. Kamego, *J.Am.Chem. Soc.*, 1975, **97**, 1163–1170.
23. F. J. Green, "*The Sigma-Aldrich Handbook of Stains, Dyes and Indicators*", Aldrich Chemical Company, Inc. Milwaukee, Wisconsin, 1990.
24. W. Khon and L. J. Sham, *Phys. Rev*., 1965, **140**, A1133.
25. G. M. Morris, R. Huey, W. Lindstrom, M. F. Sanner, R. K. Belew, D. S. Goodsell, and A. J. Olson, *J. Comput. Chem.,* 2009, **30** 2785-2791.
26. W. L. De Lano, *The PyMOL Molecular Graphics System*, De Lano Scientific, San Carlos, CA, USA, 2004.
27. Z. Yuanqin, Z. Xiancheng, Y. Xiaoqi and T. Anming, *J. Dis*. *Sci. Tech*., 1999, **20**, 437–448.
28. B. Dorrego, L. Garcia-Rio, P. Herves, J. R. Leis, J. C. Mejuto and J. Perez-Juste, *J. Phys. Chem. B*, 2001, **105***,* 4912–4920.
29. Y. Moroi, *Micelles, Theoretical and Applied Aspects*, Plenum Press, New York, 1992 (Chapter 4)
30. S. Dasmandal, H. K. Mandal, A. Kundu and A. Mahapatra, *J. Mol. Liq.,* 2014,**193**, 123–131.

31. L. Garcı´a-Rı´o, J. R. Leis, J. C. Mejuto, A. Navarro-Va´zquez, J. Pe´rez-Juste, and P. Rodriguez-Dafonte, *Langmuir*, 2004, **20**, 606-613.
32. E. Rodenas and S. Vera, *J Phys. Chem.*, 1985, **89**, 513-516.
33. C. A. Bunton, F. Nome, F. H. Quina and L. S. Romsted, *Acc. Chem. Res.* 1991, **24**, 357-364.
34. C. A. Bunton, In *Surfactants in Solution*, K. L. Mittal and D. O. Shah, Eds., Plenum Press: New York, 1991, vol. 11, p 17.
35. C. A. Bunton and G. Savelly, *Adv. Phys. Org. Chem.,* 1986, **22,** 213-309.
36. F. F. Al-Blewi, H. A. Al-Loheadan, M. Z. A. Rafiquee, Z. A. Issa, *Int. J .Chem. Kinet.* 2013, **45**, 1-9.
37. C. K. Ingold, *Structure and Mechanism in Organic Chemistry*, Bell, London, 1993.
38. R. L. VanEtten, J. F. Sevansian, G. A. Clowes and M. L. Bender, *J. Am. Chem. Soc*., 1967, **89**, 3242–3253.
39. K. N. Raymond, C. J. Hastings, M. D. Pluth and R. G. Bergman, *J. Am. Chem. Soc*., 2010, **132**, 6938–6940.
40. P. Beer, P. A. Gale and D. K. Smith, *Supramolecular Chemistry*, New York: Oxford University Press, 1999.
41. R. Breslow and S. D. Dong, *Chem. Rev*. 1998, **98**, 1997-2011.
42. M. L. Benesi and J. H. Hildebrand, *J. Am. Chem. Soc*., 1949, **71**, 2703–2707.
43. S. S. Mati, S. Sarkar, S. Rakshit, A. Sarkar and S. C. Bhattacharya, *RSC Advances*, 2013, **3**, 8071-8082.
44. A. S. Balte, P. K. Goyal and S. P. Gejji, *J. Chem. Pharm. Res*., 2012, **4**, 2391–2399.
45. *Advanced Separation Technologies Inc. in Cyclobond Handbook*, Printed in USA, 6th edn, 2002, p 1.

46. T. Lengauer and M. Rarey, *Curr. Opin. Struct. Biol.*, 1996, **6,** 402–406.

47. A. M. Vijesh, A. M. Isloor, S. Telkar, T. Arulmoli and H. K. Fun, *Arabian J. Chem.*, 2013, **6**, 197–204.